Emodin alleviates arthritis pain through reducing spinal inflammation and oxidative stress

**Ding-Wen Cheng[1,†], Yuan-Fen Yue[2,†], Chun-Xi Chen[3,†], Yin-Di Hu[1], Qiong Tang[1], Min Xie[1] , Ling Liu[1] , Dai Li[1], Hai-Li Zhu[1], and Meng-Lin Cheng[1] **

Abstract

Chronic pain is the predominant problem for rheumatoid arthritis patients, and negatively affects quality of life. Arthritis pain management remains largely inadequate, and developing new treatment strategies are urgently needed. Spinal inflammation and oxidative stress contribute to arthritis pain and represent ideal targets for the treatment of arthritis pain. In the present study, collagen-induced arthritis (CIA) mouse model was established by intradermally injection of type II collagen (CII) in complete Freund's adjuvant (CFA) solution, and exhibited as paw and ankle swelling, pain hypersensitivity and motor disability. In spinal cord, CIA inducement triggered spinal inflammatory reaction presenting with inflammatory cells infiltration, increased Interleukin-1β (IL-1β) expression, and up-regulated NOD-like receptor thermal protein domain associated protein 3 (NLRP3) and cleaved caspase-1 levels, elevated spinal oxidative level presenting as decreased nuclear factor E2-related factor 2 (Nrf2) expression and Superoxide dismutase (SOD) activity. To explore potential therapeutic options for arthritis pain, emodin was intraperitoneally injected for 3 days on CIA mice. Emodin treatment statistically elevated mechanical pain sensitivity, suppressed spontaneous pain, recovered motor coordination, decreased spinal inflammation score and IL-1β expression, increased spinal Nrf2 expression and SOD activity. Further, AutoDock data showed that emodin bind to Adenosine 5'-monophosphate (AMP)-activated protein kinase (AMPK) through two electrovalent bonds. And emodin treatment increased the phosphorylated AMPK at threonine 172. In summary, emodin treatment activates AMPK, suppresses NLRP3 inflammasome response, elevates antioxidant response, inhibits spinal inflammatory reaction and alleviates arthritis pain.

Introduction

Rheumatoid arthritis (RA) is a common systemic inflammatory autoimmune disease, and affects about 1% of the world population.[1] Chronic pain is the predominant problem for patients with RA, causes various physical and psychological impairments and negatively affects quality of life.[2] Up to 90.4% of RA patients visit a healthcare professional for intense pain[3] and have at least a 236% higher relative prevalence of functional disability.[4] Disease modifying antirheumatic drugs (DMARDs) are the mainstay of RA treatment. However, only 26% of the

[1]School of Pharmacy, Xianning Medical College, Hubei University of Science and Technology, Xianning, China
[2]Xianning Central Hospital, The First Affiliated Hospital of Hubei University of Science and Technology, Xianning, China
[3]Xishui Affiliated Hospital of Hubei University of Science and Technology, Huanggang, China

[†]These authors have contributed equally to this work

Corresponding Authors:
Meng-Lin Cheng, Xianning Medical College, Hubei University of Science and Technology, No. 88 Xianning Road, Xianning, Hubei 437100, China.
Email: menglincheng@hbust.edu.cn

Hai-Li Zhu, Xianning Medical College, Hubei University of Science and Technology, No. 88 Xianning Road, Xianning, Hubei 437100, China.
Email: hkhaili_zhu@163.com

patients were satisfied. Non-steroidal anti-inflammatory drugs (NSAIDs), opioids and glucocorticoids are common pharmacologic treatments for RA pain.[5] Due to the uncertain efficacy and overall safety of these agents, RA pain management remains largely inadequate, and many patients continue experience pain.[6] Then, illustrating the mechanisms of RA pain is useful for developing new treatment strategies.

RA pain arises from multiple mechanisms, involving joint inflammation, central sensitization and structural joint damage. Joint damage and inflammation activate and/or sensitize the primary afferents, and result in central sensitization at spinal cord level.[7] According to the central sensitization inventory, 41% of RA patients have central sensitization syndrome[8] and are associated with hyperalgesia and allodynia.[9] Central sensitization is driven by neuroinflammation, which is characterized by the activation of glial cells and the release of proinflammatory cytokines and chemokines.[10] It is reported that depending on immunomodulatory and anti-inflammatory properties, minocycline is beneficial in patients with rheumatoid arthritis.[11] And in adjuvant-induced arthritis model rats, knock-down of spinal nuclear factor-kappa B (NF-κB), a transcription factor in inflammatory reactions, reduces the overexpression of proinflammatory cytokines tumor necrosis factor α (TNFα) and interleukin-1β (IL-1β) and significantly attenuates hyperalgesia, paw edema, and joint destruction.[12] Meanwhile, oxidative stress activates cellular NF-κB inflammatory signal and leads to chronic inflammation.[13] Suppressed oxidative stress increases superoxide dismutase and catalase activity, and reduces chronic inflammatory pain in an arthritis rat model.[14] Nuclear factor erythroid 2-related factor 2 (Nrf2) is an antioxidant protein, regulates endogenous antioxidant defense and implicates in chronic inflammatory and neuropathic pain.[15] Nrf2 activation ameliorates mechanical allodynia in paclitaxel-induced neuropathic pain rats.[16] Nrf2 contributes to the anti-inflammatory process by crosstalk with the NF-κB pathway.[17] Thus, reducing oxidative stress level is an effective treatment for spinal inflammation and arthritis pain.

Emodin (1,3,8-trihydroxy-6-methylanthraquinone) is an effective constituent of the traditional Chinese medicine *Rheum palmatum* and alleviates several neuropathic pains. Emodin exhibits potent antinociceptive and anti-inflammatory effect in acetic acid, formalin, capsaicin and glutamate induced pain models.[18] In peripheral nerve chronic constriction injury model rats, emodin treatment alleviates neuropathic pain by regulating 108 differentially expressed proteins.[19] In order to explore the effect and mechanism of emodin on RA pain, arthritis pain model was established, emodin was intraperitoneally administrated on mice, and the effects of emodin on behavioral, morphological and protein expression changes were analyzed. Our study provides theoretical basis for the development of emodin as an analgesic drug for arthritis pain.

Materials and methods

Animals

A total of 30 male C57BL/6J mice weighing 18–20 g (6–8 weeks old) were purchased from Hubei Province Experimental Animal Center (Wuhan, China). All animals were housed in a 12 h light/dark circumstance with food and water ad libitum. All experimental procedures were performed according to the local and international guidelines on the ethical use of animals, and all efforts were made to minimize the number of animals used and their sufferings. Ethics approval was obtained from the Laboratory Animal Ethics Committee of Hubei University of Science and Technology (2019-03-021).

Antibodies and reagents

Cleaved caspase-1 rabbit antibody (cat# AF4022), Caspase-1 rabbit antibody (cat# AF5418), IL-1β rabbit antibody (cat# AF5103), AMPK rabbit antibody (cat# AF6423), p-AMPK rabbit antibody (cat# AF3423), NLRP3 rabbit antibody (cat# DF15549) and β-actin rabbit antibody (cat# AF7018) were obtained from Affinity Biosciences. Nrf2 rabbit polyclonal antibody (cat. no. A1244) was purchased from ABclonal Biotech Co., Ltd. H&E staining solution (cat. no. BL700 A) was purchased from Biosharp Life Sciences. Emodin (cat. B20240) was purchased from Shanghai yuanye Bio-Technology Co., Ltd. CFA (cat. P2036) was purchased from Beyotime Biotechnology. The secondary antibodies used for western blotting was HRP Goat Anti-Rabbit IgG (H + L) (AS014) purchased from ABclonal Technology. The secondary antibodies used for immunofluorescence analysis was Goat Anti-Rabbit IgG H&L (FITC) (ab6717), purchased from Abcam.

Establishment of arthritis pain model and drug administration

Mice were habituated to the environment for 5 days prior to the experiments, and randomly divided into three groups: Control, CIA and CIA + emodin. Every group contains 10 animals. 2 mg/mL bovine type II collagen (CII) solution (Chondrex, Redmond, USA, 20022) homogenized and emulsified with an equal volume of complete Freund's adjuvant (CFA). And on day 0 and day 7, 20 μL mixture were intradermally injected at the left hind paw of mice to establish collagen-induced arthritis (CIA) mouse model.[20] Paw thickness and ankle width were measured on day 14. Behaviors tests were detected on day 7 and 14.

On day 15, 16 and 17 after CIA injection, mice from CIA and CIA + emodin were intraperitoneally injected with vehicle and emodin (10 mg/kg), respectively.[21] Emodin (Shanghai yuanye Bio-Technology, China) was dissolved in DMSO and diluted with 0.9% NaCl before used.

Subsequently, behaviors tests were performed at 4 h after emodin administration. Then, all animal were scarified for further experiments after behaviors tests.

Mechanical threshold test

Mice were placed in a 30 × 30 × 30 cm plexiglass chamber and habituate for at least 30 min before behavioral experiments. The von Frey filaments (Stoelting, Wood Dale, USA, ranging from 0.008 g to 6.0 g) were used by stimulating the left hind paw. Briefly, the filaments were pressed vertically against the plantar surfaces until the filaments were bent and held for 3–5 s. At this situation, a brisk withdrawal and paw flinching was considered as positive response. Once a positive response occurred, the von Frey filament with the next lower force was applied, and whenever a negative response occurred, the filament with the next higher force was applied. Then, the pattern of positive and negative withdrawal response was converted to mechanical threshold.[22]

Spontaneous flinches test

Mice were placed in a 30 × 30 × 30 cm plexiglass chamber and habituated for at least 30 min. The number of flinches was counted sustained 5 min for three times. Take the average of the total number of flinches.[23]

Rotarod test

An accelerating rotarod was used to assess motor coordination and balance of animals. Three days before the experiment, the animals accepted acclimatization training at a fixed speed of 4 r/min for 10 min and repeat 3 times at 10-min intervals. At the beginning of experiment, the rotation speed is set at a fixed value of 10 r/min for 10 s and then accelerate for 10 s. After that, the rod is working at a speed of 20 r/min for 30 s and then accelerate for 10 s. The movement was continuously carried out for 10 min. Repeating three times with an interval of 10 min. The latency to fall of mice were recorded.[24]

H&E staining

After behaviors test, mice were deeply anesthetized with 60 mg/kg sodium pentobarbital, perfused transcardially with saline containing heparin, following with perfusing to 4% paraformaldehyde (PFA, 0.1 M phosphate buffer, pH 7.4) until the animal body was stiff and rigid. After perfusion, spinal cords were removed and post-fixed in 4% PFA for 12 h at 4°C and embedded in paraffin, and cut into 4-μm sections using a microtome (RM 2165; Leica Microsystems GmbH). The sections were stained using the standard H&E method. Briefly, sections were treated with xylene, 100% ethanol, 90% ethanol, 70% ethanol for dewaxing, dyed with hematoxylin solution, stained with eosin, sealed with neutral balsam and observed using a fluorescence microscope (Olympus IX73; Olympus). H&E images were analyzed using the ImageJ 1.51j8 software (National Institutes of Health). The scoring criteria of inflammation cell infiltration is: 0 (normal); 1 (lymphocyte infiltration around meninges and blood vessels); 2, 1-10 lymphocytes in a field); 3 (11-100 lymphocytes in a field); 4 (>100 lymphocytes in a field).

Immunofluorescence analysis

Spinal cord sections were dewaxed, conducted to antigen retrieval (Improved Citrate Antigen Retrieval Solution, P0083, Beyotime Biotechnology), treated with 3% hydrogen peroxide for 10 min, blocked with immunofluorescence blocking solution (Beyotime Biotechnology, room temperature) for 1 h, and then incubated with primary antibody overnight at 4°C, subsequently, incubated with fluorescent secondary antibody at room temperature for 1 h and observed under a fluorescence microscope (Olympus IX73; Olympus Corporation). The fluorescence intensities were analyzed using ImageJ 1.51j8 (National Institutes of Health). The following primary antibodies were used: anti-IL-1β (1:100), anti-Nrf2 (1:100), anti-NLRP3 (1:100) and anti-Caspsae-1 (1:100).

Western blotting

After behaviors test, mice were euthanized with an overdose of pentobarbital sodium (150 mg/kg) by intraperitoneal injection and sacrificed through decapitation. Lumber spinal cord samples were collected, homogenized in RIPA lysis buffer containing 1% protease inhibitors (Sigma-Aldrich; Merck KGaA), centrifugated at 12,000 g, 4°C for 20 min. Then the supernatant was collected, separated on SDS-PAGE, and transferred to 0.22 μm PVDF membranes. Protein concentration was quantified using a BCA analysis kit (Beyotime Biotechnology). Then the membranes were blocked with QuickBlockTM Blocking Buffer for Western Blot (Beyotime, China), incubated with the appropriate primary antibodies overnight at 4°C. And HRP-conjugated secondary antibodies in TBST (1:5,000) at room temperature for 1 h. Protein bands were visualized using ECL detection reagent (Biosharp Life Sciences) and detected with an iBright 1500 instrument (Invitrogen; Thermo Fisher Scientific, Inc.). The grey values of bands were analyzed using ImageJ 1.51j8 software (National Institutes of Health). β-actin was used as a loading control. The following primary antibodies were used: anti-IL-1β (1:1000), anti-Nrf2 (1:1000), anti-AMPK (1:1000), Anti-pAMPK (1:1000), anti-NLRP3 (1:1000) and anti-Cleaved-Caspsae-1 (1:1000).

Molecular docking

The X-ray crystal structure of AMPK was obtained from the Protein Data Bank (PDB ID: 4EAI https://www.rcsb.org/). The structure of emodin was downloaded from the PubChem database (https://www.pubchem.ncbi.nlm.nih.gov/compound) and optimized using ChemBio3D Ultra 14.0 software (PerkinElmer Informatics). Auto Dock Vina 1.2.0 software (Center for Computational Structural Biology) was used to dock conformation between AMPK and emodin. PyMOL 2.2.3 was used to visualize the conformation.[25]

Measurement of superoxide dismutase activity

For determination of superoxide dismutase (SOD) enzyme activity, Cu/Zn-SOD and Mn-SOD assay kit with WST-8 (Beyotime, Shanghai, China) was prepared. Briefly, spinal cords were homogenized in ice-cold Phosphate Buffered Saline (PBS) buffer, centrifuged at 12,000 g for 15 min, and the supernatant was collected and mixed with WST-8 enzyme working solution for 20 min at 37°C, the OD_{450nm} absorbance value of each pore was measured. SOD activity was expressed as units per milligram of total protein (U/mg protein).

Statistical analysis

All statistical analyses were performed using SPSS 26.0 statistics software (IBM Corp.). A paired samples *t*-test was used to compare the means of paw thickness and ankle width. Data of behaviors tests were analyzed using one-way analysis of variance followed by Tukey's test. Data for H&E staining, immunofluorescence and western blotting were presented as the mean ± SD. Data for behaviors tests were presented as the mean ± SEM. $p < 0.05$ was considered to indicate a statistically significant difference.

Results

Emodin treatment relieves pain hypersensitivity of CIA mice

Behaviors tests were performed following protocol as shown in Figure 1(a). As shown in Figure 1(b), on day 14, CIA inducement leads to a swelling of paw and ankle. The paw thickness of mice in control group was at 2.54 ± 0.11, while in CIA group at 3.81 ± 0.09 ($p < 0.05$ vs. control group) (Figure 1c). The ankle width of mice in control group was at 2.72 ± 0.04, while in CIA group at 3.67 ± 0.10 ($p < 0.05$ vs. control group) (Figure 1d). Meanwhile, compared with control group, mechanical threshold values presenting mechanical pain sensitivity were significantly decreased in CIA mice from 1.26 ± 0.08 (day 0) to 0.44 ± 0.09 (day 7, $p < 0.05$), 0.35 ± 0.04 (day 14, $p < 0.05$). Numbers of flinches presenting spontaneous pain were dramatically increased in CIA mice from 3.22 ± 0.40 (day 0) to 11.56 ± 1.04 (day 7, $p < 0.05$), 13.11 ± 0.86 (day 14, $p < 0.05$). Latency to fall presenting
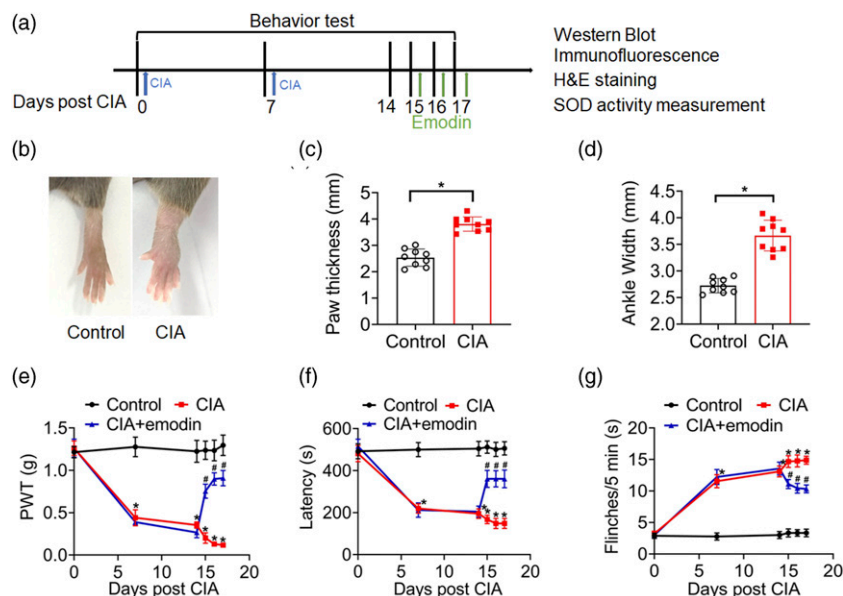

Figure 1. Effect of emodin treatment on pain behaviors of CIA mice. (a) Schematic diagram of the experimental procedures. On day 0 and 7, CII in CFA solution were injected on mice, and behavior test were conducted at day 0, 7, and 14. Emodin was intraperitoneally injected on mice on day 15, 16 and 17. And after 4 h of emodin treatment, behavior tests were conducted. Subsequently mice were sacrificed and spinal cord tissues were collected for the further analysis. (b) Representative images of the left hind paw from control and CIA mice on day 14 after CIA inducement. (c, d) Changes of paw thickness (c) and ankle width (d) from control and CIA mice on day 14 after CIA inducement. (e–g) Changes of PWT values (e), spontaneous flinches (f) and latency to fall (g) of mice. Data are expressed as the mean ± SEM ($n = 9$ mice/group). *$p < 0.05$ vs. control group, #$p < 0.05$ vs. CIA group.

motor coordination were reduced in CIA mice from 481.16 ± 38.49 (day 0) to 220.00 ± 22.49 (day 7, $p < 0.05$), and 195.48 ± 22.81 (day 14, $p < 0.05$). These data revealed that pain hypersensitivity and motor disability were induced on CIA mice. Further, after emodin treatment on day 15, 16 and 17, mechanical threshold values of mice in CIA + emodin group were statistically raised to 0.75 ± 0.08, 0.90 ± 0.07 and 0.91 ± 0.09, respectively ($p < 0.05$ vs. CIA group) (Figure 1e). Flinches numbers of mice in CIA + emodin group were obviously descended to 11.11 ± 0.72, 10.44 ± 0.77 and 10.33 ± 0.62, respectively ($p < 0.05$ vs CIA group) (Figure 1f). Latency to fall of mice in CIA + emodin group were apparently increased to 360.54 ± 40.78, 361.26 ± 38.32 and 360.62 ± 42.23, respectively ($p < 0.05$ vs. CIA group) (Figure 1g). Then, emodin treatment elevated mechanical pain sensitivity, suppressed spontaneous pain and recovered motor coordination of CIA mice.

Emodin treatment decreases spinal inflammation

Detecting by H&E staining, severe infiltration of inflammatory cells (red arrow) was observed in the spinal dorsal horn of CIA mice ($p < 0.05$ vs. control group), while emodin treatment decreased the inflammatory response induced by CIA administration ($p < 0.05$ vs. CIA group) (Figure 2a).

The relative inflammation scores in the CIA and CIA + emodin groups were 2.54 ± 0.12 and 2.26 ± 0.10, respectively (Figure 2b). Meanwhile the expression levels of IL-1β were detected. Compared with control group, the fluorescence intensity of IL-1β in spinal dorsal horn of CIA group was significantly enhanced ($p < 0.05$), and Emodin treatment down-regulated IL-1β intensity ($p < 0.05$ vs. CIA group) (Figure 2c). Relative intensity of IL-1β in CIA and CIA + emodin groups were 1.57 ± 0.10 and 1.22 ± 0.13, (Figure 2d). Western blotting showed (Figure 2e) that the expression level of spinal IL-1β in CIA mice was increased to 1.54 ± 0.30 ($p < 0.05$ vs. control group). Emodin treatment down-regulated IL-1β expression levels to 1.03 ± 0.16 ($p < 0.05$ vs. CIA group) (Figure 2f).

Emodin treatment inhibits spinal NLPR3 inflammasome activity

NLRP3 inflammasome mediates caspase-1 activation and IL-1β secretion.[26] The fluorescence intensity of NLRP3 and caspase-1 in spinal dorsal horn was increased in the CIA group (Figure 3a and c) with a relative intensity of 1.44 ± 0.09 and 1.48 ± 0.06, respectively ($p < 0.05$ vs. control group, Figure 3b and d). Emodin treatment reduced the intensity of NLRP3 and caspase-1 to 1.18 ± 0.09 and 1.20 ± 0.06,
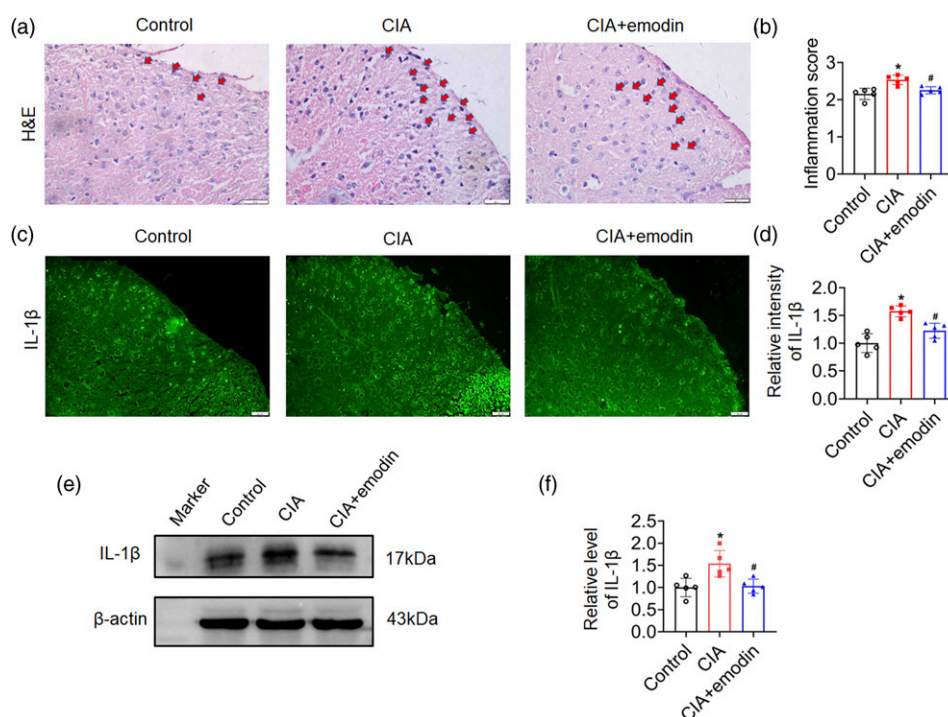

Figure 2. Effect of emodin treatment on spinal inflammatory infiltration and IL-1β expression. (a) Representative H&E staining images of spinal cord sections from control, CIA and CIA + emodin groups. Scale bar = 20 μm. (b) Quantitative analysis of inflammation score for the H&E staining in each group. (c, d) Representative immunofluorescence staining images of IL-1β expressions in spinal dorsal horn (c) and quantitative fluorescence intensity analysis (d). Scale bar = 20 μm. (e, f) Western blot analysis (e) and quantification of the relative grey value (f) of IL-1β expression level in spinal cord of control, CIA and CIA + emodin groups. Data are presented as mean ± SD (n = 5 mice/group). *p < 0.05 vs. control group, #p < 0.05 vs. CIA group.

respectively ($p < 0.05$ vs. control group, Figure 3b and d) While, western blot analysis showed that spinal expression of NLRP3 and cleaved caspase-1 were up-regulated in CIA group ($p < 0.05$ vs. control group, Figure 3e), and the relative grey values were 1.53 ± 0.11 and 2.37 ± 0.37, respectively. Emodin treatment down-regulated the expression levels of NLRP3 and activated caspase-1 to 1.22 ± 0.18 and 1.66 ± 0.44, respectively ($p < 0.05$ vs. CIA group, Figure 3f).

Emodin treatment reduces spinal oxidative levels

The antioxidant response element Nrf2 level was detect. And as shown in Figure 4(a), the fluorescence intensity of Nrf2 in spinal dorsal horn was decreased in the CIA group, with a relative intensity of 0.75 ± 0.05 ($p < 0.05$ vs. control group, Figure 4b). Emodin treatment increased the intensity of Nrf2 to 0.86 ± 0.03 ($p < 0.05$ vs. CIA group, Figure 4b). While,
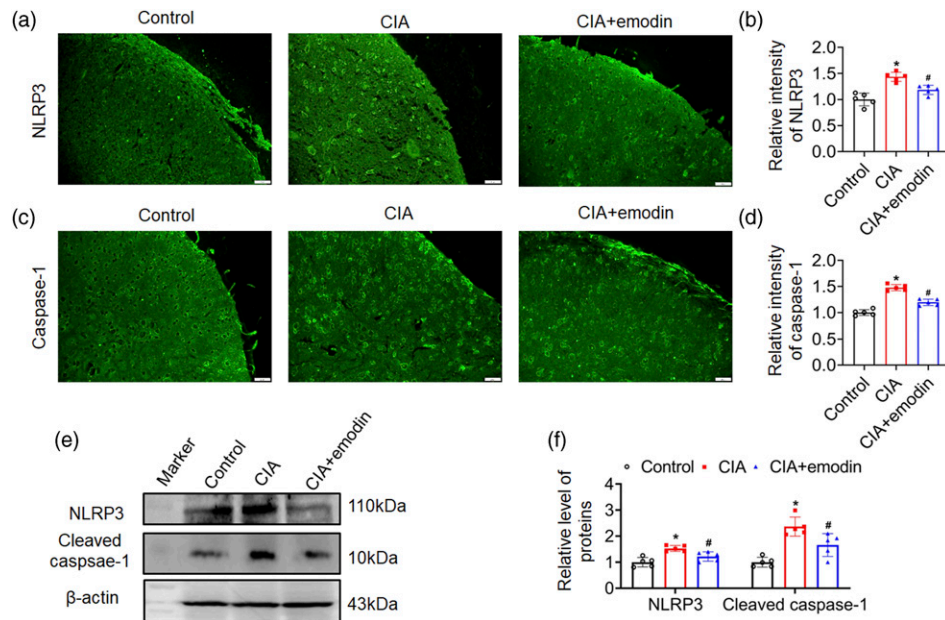

Figure 3. Effect of emodin treatment on NLRP3 inflammasome components. (a, c) Representative immunofluorescence staining images show the expressions of NLRP3 and caspase-1 in spinal dorsal horn of control, CIA and CIA + emodin groups. Scale bar = 20 μm. (b, d) Quantitative analysis of fluorescence intensity of NLRP3 and caspase-1. (e–f) Western blot analysis (e) and relative grey values (f) of expression levels of NLRP3 and activated casepase-1 in spinal cord of control, CIA and CIA + emodin groups. β-actin was used as a loading control. Data are presented as mean ± SD ($n = 5$ mice/group). *$p < 0.05$ vs. control group, #$p < 0.05$ vs. CIA group.
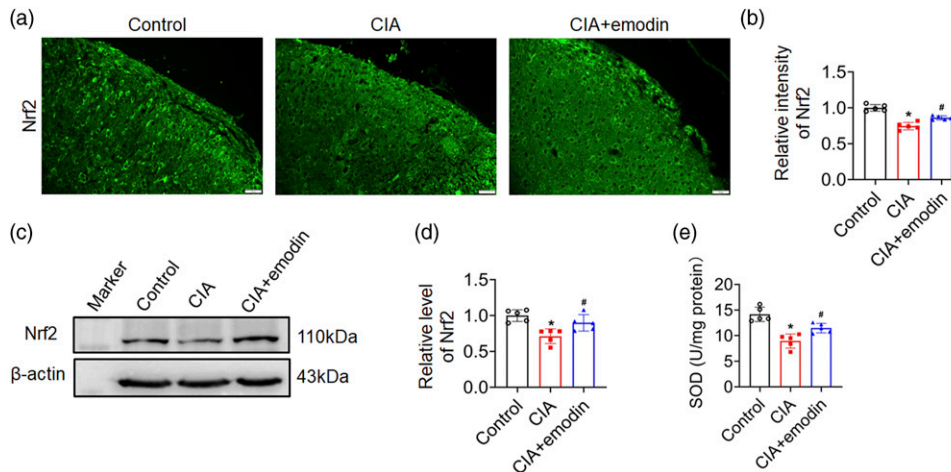

Figure 4. Effect of emodin treatment on oxidative level. (a, b) Representative immunofluorescence staining images (a) and quantitative intensity analysis (b) of Nrf2 in spinal dorsal horn of control, CIA and CIA + emodin groups. Scale bar = 20 μm. (c, d) Western blot analysis (c) and relative grey values (d) of expression levels of Nrf2 in spinal cord. β-actin was used as a loading control. (e) Reagent test kit assay for SOD activity in spinal cord of mice. Data are presented as mean ± SD ($n = 5$ mice/group). *$p < 0.05$ vs. control group, #$p < 0.05$ vs. CIA group.

western blot analysis showed that spinal expression of Nrf2 was down-regulated in CIA group (Figure 4c), with the relative grey values as 0.71 ± 0.10 ($p < 0.05$ vs. control group, Figure 4d). Emodin treatment up-regulated the expression level of Nrf2 to 1.08 ± 0.11 ($p < 0.05$ vs. CIA group, Figure 4d). Meanwhile, Superoxide dismutase (SOD) is an important enzyme in controlling of ROS.[27] And as shown in Figure 4(e), SOD activity in control group was 14.16 ± 1.40 U/mg, however, in CIA group was suppressed to 8.94 ± 1.38 U/mg ($p < 0.05$ vs. control group). Emodin treatment increased the activity to 11.46 ± 0.93 U/mg ($p < 0.05$ vs. CIA group).

Emodin treatment decreases spinal AMPK expression and activity

A molecular docking assay was performed on the X-ray crystal structures of AMPK and the ligand emodin (Figure 5a–c). Auto Dock data showed that emodin formed two electrovalent bonds with AMPK at residues Lys-60 and Asn-162. The electrovalent bond distances were measured to be 2.2 ngstrom between AMPK Lys-60 and emodin, and 2.2 ngstrom between AMPK Asn-162 and emodin. And the binding affinity was -7.7 kcal/mol. Meanwhile, the effect of emodin on AMPK expression and activity were detected by western blot analysis. Western blot analysis indicated that p-AMPK-Thr172 level was down-regulated in the CIA

group (Figure 5d) showing a relative gray value of 0.54 ± 0.14 ($p < 0.05$ vs. control group, Figure 5e). The pAMPK-Thr174 expression was enhanced following emodin treatment in CIA + emodin group (Figure 5d), with a relative gray value increased to 0.82 ± 0.06 ($p < 0.05$ vs. CIA group, Figure 5e).

Discussion

In our study, we found that emodin activated AMPK and alleviated arthritis pain. AMPK, as a serine/threonine kinase, is associated with various types of pain and is a potential target for pain management.[28] AMPK activation by AICAR, metformin and resveratrol phosphorylated at Thr172, resultes in 1000-fold activation of AMPK activity, and alleviates inflammatory pain, nerve injury, painful diabetic neuropathy and cancer pain in experimental animal models.[29,30] In CIA induced inflammatory pain model mice, AMPK activator AICAR produces an analgesic effect and inhibits the level of proinflammatory cytokine IL-1β. While, AMPK inhibitor Compound C and AMPKα shRNA reverses the analgesic effect and IL-1β and NF-κB activation.[31] In osteoarthritis model mice, berberine induces phosphorylation of AMPKα (Thr172), significantly reduces severity of osteoarthritis and associated pain, but not affects in AMPKα1-knockout mice.[32] Meanwhile, emodin activates AMPK in both 3T3-L1
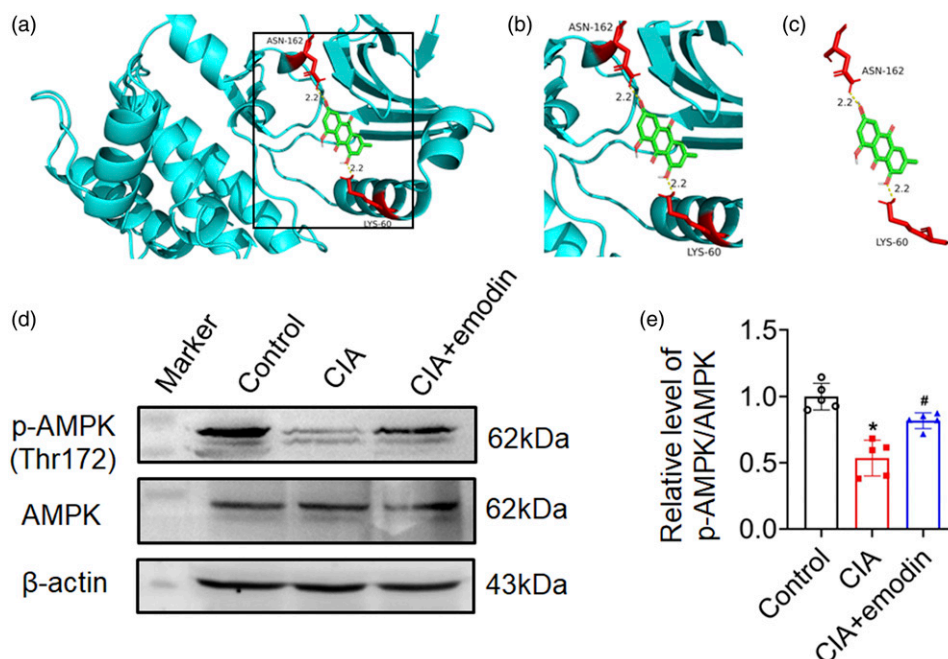

Figure 5. Effect of emodin treatment on AMPK activity. (a–c) the docking results of emodin with AMPK. The modelled 3D structure of AMPK docked with emodin (a). The enlarged view of binding site in box (b). The interaction bonds of AMPK with emodin (c). AMPK protein was shown in color cyan. Emodin was colored green. The interaction residues showed as color red, bonds showed as yellow dotted lines, and bond lengths were presented as numbers. (d, e) Western blot analysis (d) and quantification of the relative grey value (e) of phosphorylated AMPK (Thr172) level in spinal cord of control, CIA and CIA + emodin groups. Data are presented as mean ± SD ($n = 5$ mice/group). *$p < 0.05$ vs. control group, #$p < 0.05$ vs. CIA group.

adipocytes and 293T cells.[33] In liver inflammation model mice, emodin increases AMPK/Yes-associated protein 1 (YAP1) pathway and inhibits oxidative liver injury.[34] In diabetic nephropathy (DN) podocyte injury model rats, emodin enhances autophagy of podocytes via the AMPK/mTOR signaling pathway.[35] In this study, we found that emodin bind with AMPK at −7.7 kcal/mol binding affinity which presented a relatively stable docking result.[36] Meanwhile, our data showed that emodin activated AMPK in spinal cord of CIA mice. Then, we suggested that emodin alleviated arthritis pain via binding with AMPK and promoting its activity.

AMPK regulates inflammation and oxidative stress trough several pathways. It was reported that AMPK phosphorylation modulates pain by activation of NLRP3 inflammasome. Deficient AMPK activation and overactivation of NLRP3 inflammasome axis are observed in blood cells from patients with fibromyalgia. AMPK inhibitors compound Cor sunitinib treatment impaires AMPK activation, activates NLRP3 inflammasome, increases serum levels of IL-1β, and provokes hyperalgesia in mice.[37,38] In the pathophysiology of aging and age-related diseases, NLRP3 inflammasome is regulated by AMPK-dependent pathways.[39] In spinal cord injury model rats, metformin treatment activates AMPK phosphorylation, reduces NLRP3 inflammasome activation and reduces proinflammatory cytokine (IL-1β, IL-6, and TNF-α) release.[40] AMPK also phosphorylates Nrf2 at the Ser558 residue and causes Nrf2 nuclear accumulation, and promotes antioxidant response.[41] In BV-2 cells and primary cultured microglia, Nrf2 knockdown by shRNA exacerbates NaF-induced oxidative stress and inflammation. While, AMPK deletion by siRNA blocks the activating effect of NaF on Nrf2.[42] In lipopolysaccharide (LPS)-triggered inflammatory system, Nrf2 is activated in AMPK-dependent manner. And pharmacologically or genetically inactivating AMPK blocks the activation of Nrf2.[43] Further, Nrf2 is essential for inflammasome activation. Nrf2 is required for NLRP3 activators to promote IL-1β secretion via ASC speck formation.[44] Nrf2-deficient macrophages show decreased maturation and secretion of caspase-1 and IL-1β and reduced NLRP3 inflammasome stimuli.[45,46] In our study, we found emodin activated AMPK, increased Nrf2 expression and inhibited NLRP3 inflammasome activation. Combining our data, it was considered that emodin suppressed spinal inflammation via activating AMPK-Nrf2 pathway.
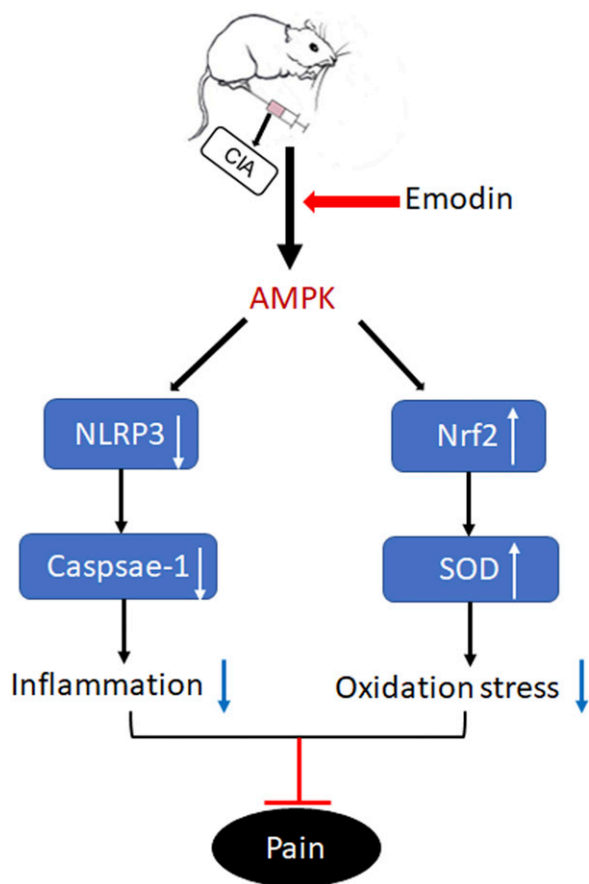

Figure 6. Schematic representation of the potential mechanisms of emodin treatment on alleviating arthritis pain.

Conclusion

During arthritis processing, spinal inflammatory reaction was activated, spinal oxidative stress was increased. Emodin treatment activated spinal AMPK, increased Nrf2-mediated antioxidant response, suppressed spinal NLRP3 mediated inflammatory reaction, and alleviated arthritis pain (Figure 6).

Author contributions

M-LC conceived and designed the study. D-WC, Y-FY, Y-DH, C-XC, QT, and LL acquired, analyzed, and interpreted the data. H-LZ and MX drafted and edited the manuscript. DL and M-LC made the revision. All authors aided in revising this manuscript for intellectual content and approved the final version to be published.

Declaration of conflicting interests

The author(s) declared no potential conflicts of interest with respect to the research, authorship, and/or publication of this article.

Funding

Data availability statement

The data sets used and analyzed during the current study are available from the corresponding author on reasonable request.

ORCID iDs

Min Xie ⓘ https://orcid.org/0000-0002-0029-0496
Ling Liu ⓘ https://orcid.org/0000-0002-7016-2713
Meng-Lin Cheng ⓘ https://orcid.org/0000-0002-4679-6329

References

1. Almutairi KB, Nossent JC, Preen DB, Keen HI, Inderjeeth CA. The prevalence of rheumatoid arthritis: A systematic review of population-based studies. *J Rheumatol* 2021; 48: 669–676.

2. Mathias K, Amarnani A, Pal N, Karri J, Arkfeld D, Hagedorn JM, Abd-Elsayed A. Chronic pain in patients with rheumatoid arthritis. *Curr Pain Headache Rep* 2021; 25: 59.

3. De Cock D, Van der Elst K, Stouten V, Peerboom D, Joly J, Westhovens R, Verschueren P. The perspective of patients with early rheumatoid arthritis on the journey from symptom onset until referral to a rheumatologist. *Rheumatol Adv Pract* 2019; 3: rkz035.

4. Lo J, Chan L, Flynn S. A systematic review of the incidence, prevalence, costs, and activity and work limitations of amputation, osteoarthritis, rheumatoid arthritis, back pain, multiple sclerosis, spinal cord injury, stroke, and traumatic brain injury in the United States: A 2019 update. *Arch Phys Med Rehabil* 2021; 102: 115–131.

5. Sanchez-Florez JC, Seija-Butnaru D, Valero EG, Acosta C, Amaya S. Pain management strategies in rheumatoid arthritis: A narrative review. *J Pain Palliat Care Pharmacother* 2021; 35: 291–299.

6. Cao Y, Fan D, Yin Y. Pain mechanism in rheumatoid arthritis: from cytokines to central sensitization. *Mediators Inflamm* 2020; 2020: 2076328.

7. Zhang A, Lee YC. Mechanisms for joint pain in rheumatoid arthritis (RA): from cytokines to central sensitization. *Curr Osteoporos Rep* 2018; 16: 603–610.

8. Guler MA, Celik OF, Ayhan FF. The important role of central sensitization in chronic musculoskeletal pain seen in different rheumatic diseases. *Clin Rheumatol* 2020; 39: 269–274.

9. Salaffi F, Di Carlo M, Carotti M, Sarzi-Puttini P. The effect of neuropathic pain symptoms on remission in patients with early rheumatoid arthritis. *Curr Rheumatol Rev* 2019; 15: 154–161.

10. Ji RR, Nackley A, Huh Y, Terrando N, Maixner W. Neuroinflammation and central sensitization in chronic and widespread pain. *Anesthesiology* 2018; 129: 343–366.

11. Langevitz P, Livneh A, Bank I, Pras M. Benefits and risks of minocycline in rheumatoid arthritis. *Drug Saf* 2000; 22: 405–414.

12. Luo JG, Zhao XL, Xu WC, Zhao XJ, Wang JN, Lin XW, Sun T, Fu ZJ. Activation of spinal NF-kappaB/p65 contributes to peripheral inflammation and hyperalgesia in rat adjuvant-induced arthritis. *Arthritis Rheumatol* 2014; 66: 896–906.

13. Reuter S, Gupta SC, Chaturvedi MM, Aggarwal BB. Oxidative stress, inflammation, and cancer: how are they linked? *Free Radic Biol Med* 2010; 49: 1603–1616.

14. Zhou SZ, Zhou YL, Ji F, Li HL, Lv H, Zhang Y, Xu H. Analgesic effect of methane rich saline in a rat model of chronic inflammatory pain. *Neurochem Res* 2018; 43: 869–877.

15. Zhou YQ, Mei W, Tian XB, Tian YK, Liu DQ, Ye DW. The therapeutic potential of Nrf2 inducers in chronic pain: evidence from preclinical studies. *Pharmacol Ther* 2021; 225: 107846.

16. Zhou YQ, Liu DQ, Chen SP, Chen N, Sun J, Wang XM, Cao F, Tian YK, Ye DW. Nrf2 activation ameliorates mechanical allodynia in paclitaxel-induced neuropathic pain. *Acta Pharmacol Sin* 2020; 41: 1041–1048.

17. Ahmed SM, Luo L, Namani A, Wang XJ, Tang X. Nrf2 signaling pathway: Pivotal roles in inflammation. *Biochim Biophys Acta Mol Basis Dis* 2017; 1863: 585–597.

18. Zhang X, Li J, Guan L. Emodin reduces inflammatory and nociceptive responses in different pain and inflammation-induced mouse models. *Comb Chem High Throughput Screen* 2022.

19. Chen P, Lin D, Wang C, Song C, Wang W, Qu J, Wu Z. Proteomic analysis of emodin treatment in neuropathic pain reveals dysfunction of the calcium signaling pathway. *J Pain Res* 2021; 14: 613–622.

20. Angeby Moller K, Svard H, Suominen A, Immonen J, Holappa J, Stenfors C. Gait analysis and weight bearing in pre-clinical joint pain research. *J Neurosci Methods* 2018; 300: 92–102.

21. Hashida R, Shimozuru Y, Chang J, Agosto-Marlin I, Waritani T, Terato K. New studies of pathogenesis of rheumatoid arthritis with collagen-induced and collagen antibody-induced arthritis models: new insight involving bacteria flora. *Autoimmune Dis* 2021; 2021: 7385106.

22. Hao M, Tang Q, Wang B, Li Y, Ding J, Li M, Xie M, Zhu H. Resveratrol suppresses bone cancer pain in rats by attenuating inflammatory responses through the AMPK/Drp1 signaling. *Acta Biochim Biophys Sin (Shanghai)* 2020; 52: 231–240.

23. Mao Y, Wang C, Tian X, Huang Y, Zhang Y, Wu H, Yang S, Xu K, Liu Y, Zhang W, Gu X, Ma Z. Endoplasmic reticulum stress contributes to nociception via neuroinflammation in a murine bone cancer pain model. *Anesthesiology* 2020; 132: 357–372.

24. Shi X, Bai H, Wang J, Wang J, Huang L, He M, Zheng X, Duan Z, Chen D, Zhang J, Chen X, Wang J. Behavioral assessment of sensory, motor, emotion, and cognition in rodent models of intracerebral hemorrhage. *Front Neurol* 2021; 12: 667511.

25. Seeliger D, de Groot BL. Ligand docking and binding site analysis with PyMOL and Autodock/Vina. *J Comput Aided Mol Des* 2010; 24: 417–422.

26. Zhang T, Du H, Feng S, Wu R, Chen T, Jiang J, Peng Y, Ye C, Fang R. NLRP3/ASC/Caspase-1 axis and serine protease activity are involved in neutrophil IL-1beta processing during Streptococcus pneumoniae infection. *Biochem Biophys Res Commun* 2019; 513: 675–680.

27. Younus H. Therapeutic potentials of superoxide dismutase. *Int J Health Sci (Qassim)* 2018; 12: 88–93.

28. Wang S, Dai Y. Roles of AMPK and its downstream signals in pain regulation. *Life (Basel)* 2021; 11.

29. Steinberg GR, Carling D. AMP-activated protein kinase: the current landscape for drug development. *Nat Rev Drug Discov* 2019; 18: 527–551.

30. Zhang J, Wang Y, Bao C, Liu T, Li S, Huang J, Wan Y, Li J. Curcuminloaded PEGPDLLA nanoparticles for attenuating palmitateinduced oxidative stress and cardiomyocyte apoptosis through AMPK pathway. *Int J Mol Med* 2019; 44: 672–682.

31. Shi M, Wang J, Xiao Y, Wang C, Qiu Q, Lao M, Yu Y, Li Z, Zhang H, Ye Y, Liang L, Yang X, Chen G, Xu H. Glycogen metabolism and rheumatoid arthritis: The role of glycogen synthase 1 in regulation of synovial inflammation via blocking AMP-activated protein kinase activation. *Front Immunol* 2018; 9: 1714.

32. Li J, Wang Y, Chen D, Liu-Bryan R. Oral administration of berberine limits post-traumatic osteoarthritis development and associated pain via AMP-activated protein kinase (AMPK) in mice. *Osteoarthritis Cartilage* 2022; 30: 160–171.

33. Chen Z, Zhang L, Yi J, Yang Z, Zhang Z, Li Z. Promotion of adiponectin multimerization by emodin: a novel AMPK activator with PPARgamma-agonist activity. *J Cell Biochem* 2012; 113: 3547–3558.

34. Lee EH, Baek SY, Park JY, Kim YW. Emodin in Rheum undulatum inhibits oxidative stress in the liver via AMPK with Hippo/Yap signalling pathway. *Pharm Biol* 2020; 58: 333–341.

35. Liu H, Wang Q, Shi G, Yang W, Zhang Y, Chen W, Wan S, Xiong F, Wang Z. Emodin ameliorates renal damage and podocyte injury in a rat model of diabetic nephropathy via regulating AMPK/mTOR-mediated autophagy signaling pathway. *Diabetes Metab Syndr Obes* 2021; 14: 1253–1266.

36. Dutta M, Tareq AM, Rakib A, Mahmud S, Sami SA, Mallick J, Islam MN, Majumder M, Uddin MZ, Alsubaie A, Almalki ASA, Khandaker MU, Bradley DA, Rana MS, Emran TB. Phytochemicals from Leucas zeylanica targeting main protease of SARS-CoV-2: Chemical profiles, molecular docking, and molecular dynamics simulations. *Biology (Basel)* 2021.

37. Bullon P, Alcocer-Gomez E, Carrion AM, Marin-Aguilar F, Garrido-Maraver J, Roman-Malo L, Ruiz-Cabello J, Culic O, Ryffel B, Apetoh L, Ghiringhelli F, Battino M, Sanchez-Alcazar JA, Cordero MD. AMPK phosphorylation modulates pain by activation of NLRP3 inflammasome. *Antioxid Redox Signal* 2016; 24: 157–170.

38. Zhang YZ, Zhang YL, Huang Q, Huang C, Jiang ZL, Cai F, Shen JF. AdipoRon alleviates free fatty acid-induced myocardial cell injury via suppressing Nlrp3 inflammasome activation. *Diabetes Metab Syndr Obes* 2019; 12: 2165–2179.

39. Cordero MD, Williams MR, Ryffel B. AMP-activated protein kinase regulation of the NLRP3 inflammasome during aging. *Trends Endocrinol Metab* 2018; 29: 8–17.

40. Yuan Y, Fan X, Guo Z, Zhou Z, Gao W. Metformin Protects against Spinal Cord Injury and Cell Pyroptosis via AMPK/NLRP3 Inflammasome Pathway. *Anal Cell Pathol (Amst)* 2022; 2022: 3634908.

41. Joo MS, Kim WD, Lee KY, Kim JH, Koo JH, Kim SG. AMPK facilitates nuclear accumulation of Nrf2 by phosphorylating at serine 550. *Mol Cell Biol* 2016; 36: 1931–1942.

42. Song C, Heping H, Shen Y, Jin S, Li D, Zhang A, Ren X, Wang K, Zhang L, Wang J, Shi D. AMPK/p38/Nrf2 activation as a protective feedback to restrain oxidative stress and inflammation in microglia stimulated with sodium fluoride. *Chemosphere* 2020; 244: 125495.

43. Mo C, Wang L, Zhang J, Numazawa S, Tang H, Tang X, Han X, Li J, Yang M, Wang Z, Wei D, Xiao H. The crosstalk between Nrf2 and AMPK signal pathways is important for the anti-inflammatory effect of berberine in LPS-stimulated macrophages and endotoxin-shocked mice. *Antioxid Redox Signal* 2014; 20: 574–588.

44. Jhang JJ, Yen GC. The role of Nrf2 in NLRP3 inflammasome activation. *Cell Mol Immunol* 2017; 14: 1011–1012.

45. Zhao C, Gillette DD, Li X, Zhang Z, Wen H. Nuclear factor E2-related factor-2 (Nrf2) is required for NLRP3 and AIM2 inflammasome activation. *J Biol Chem* 2014; 289: 17020–17029.

46. Li MY, Ding JQ, Tang Q, Hao MM, Wang BH, Wu J, Yu LZ, Jiao M, Luo BH, Xie M, Zhu HL. SIRT1 activation by SRT1720 attenuates bone cancer pain via preventing Drp1-mediated mitochondrial fission. *Biochim Biophys Acta Mol Basis Dis* 2019; 1865: 587–598.